Nonlinear Control Experiments on an Axial Flow Compressor*

Dan Fontaine† dan@seidel.ece.ucsb.edu
Shengfang Liao‡ sliao@mit.edu
James Paduano‡ paduano@mit.edu
Petar Kokotović† petar@ece.ucsb.edu

Abstract

A nonlinear control law is designed for a low order model of an axial flow compressor with a ring of bleed valves after the last compressor stage. The controller is implemented on a low speed, three stage experimental compressor. The region of attraction guaranteed by the control law is experimentally determined and is larger than that of the uncontrolled compressor.

1 Introduction

Several experiments in the control of axial flow compressors have been reported in recent years. Paduano *et al* [1, 2] used inlet guide vanes for the control of rotating stall. Air injection control experiments by Freeman *et al* [3] showed the potential for a significant increase of the stable operating range of a Rolls-Royce Viper turbojet. Other air injection controllers have been tested by Weigl *et al* [4], Protz [5], D'Andrea *et al* [6] and Wang *et al* [7]. Control with bleed valves at the throttle end of the compressor was used in experiments by Eveker *et al* [8] and Badmus *et al* [9]. Yeung, Behnken and Murray [10, 11] implemented a controller with air injection for stall control and bleed valves for surge control. Other experimental studies are surveyed by Willems and Jager [12].

The influence of air injectors on both the axial (1D) and circumferential dimensions (2D) of the mass flow is faster than bleed actuation at the throttle end of the compressor. However, bleed valves are much easier to implement and are more likely to be incorporated in commercial aeroengines. To combine the relative simplicity of bleed actuation with the 2D control authority of air injection, Fontaine *et al* [13] designed a nonlinear control law for actuation with a ring of bleed valves placed near the compressor stages. This paper reports on the implementation and experimental evaluation of this control law.

Two of the the most common causes of instability in industrial turbomachines are acceleration and inlet distortion. As described in Kerrebrock [14], acceleration increases the fuel flow, causes an increase in temperature, and a decrease in pressure. The pressure drop may reduce the mass flow rate into a region where steady state operation is unstable. Inlet distortion causes a non-axisymmetric flow in the compressor. Hynes and Greitzer [15] described how reduced mass flow from distortion can trigger rotating stall and/or surge. Thus, both acceleration and distortion cause temporary excursions outside the region where stable steady state operation is possible.

To improve engine operability, a feedback controller must be capable of returning the compressor to a stable steady state. A criterion that assesses this ability is the region of attraction guaranteed by the controller. This region is the set of compressor states which will return to the equilibrium represented by the desired steady state. The highest pressure rise is achieved at the peak of its steady state characteristic. Our goal is to stabilize this equilibrium and provide the largest possible region of attraction.

We report on experiments with the LS3 compressor in the Gas Turbine Laboratory at the Massachusetts Institute of Technology. The LS3 is a three stage, low speed compressor equipped with a ring of bleed valves after the last stage of the compressor. We discuss the properties of a low

*Research supported in part by the National Science Foundation under grant ECS-9812346 and the Air Force Office of Scientific Research under grant F49620-95-1-0409.

†Center for Control Engineering and Computation, University of California at Santa Barbara

‡Gas Turbine Laboratory, Massachusetts Institute of Technology

order compressor model in Section 2 and we use it to design a nonlinear control law in Section 3. The experimental facility is described in Section 4 and controller implementation is presented in Section 5. Our experimental results are summarized in Section 6, where we contrast the region of attraction guaranteed by the controller with that of the uncontrolled compressor.

2 Properties of a 2D Downstream Bleed Model

Many recent compressor control studies have utilized low order approximations of the Moore-Greitzer [16] PDE model. Its single mode approximation is extended [13] for 2D interstage bleed by including the effects of the bleed valves on the mass flow balance and pressure balance. The parameter α denotes bleed anywhere from the first compressor stage ($\alpha = 1$) to the last ($\alpha = 0$). For the bleed implemented at the last stage of the LS3 experimental compressor, α is set to zero and the model [13] becomes

$$\begin{aligned}
\dot{\Phi} &= \frac{1}{l_c}\left[\psi_c(\Phi) + \frac{1}{4}\psi_c''(\Phi)(a^2+b^2) - \Psi \right. \\
&\quad \left. + \Phi\bar{\Phi}_b + \frac{1}{2}(aC_a + bC_b)\right] \qquad (2.1)\\
\dot{\Psi} &= \frac{1}{4l_cB^2}\left[\Phi - \bar{\Phi}_b - \sqrt{\frac{2\Psi}{K_T}}\right] \qquad (2.2)\\
\dot{a} &= \left[\left((\psi_c'(\Phi) + \frac{1}{8}\psi_c'''(a^2+b^2) + \bar{\Phi}_b\right)a \right. \\
&\quad \left. + \Phi C_a - \lambda b\right]\frac{1}{\mu+m} \qquad (2.3)\\
\dot{b} &= \left[\left((\psi_c'(\Phi) + \frac{1}{8}\psi_c'''(a^2+b^2) + \bar{\Phi}_b\right)b \right. \\
&\quad \left. + \Phi C_b + \lambda a\right]\frac{1}{\mu+m} \qquad (2.4)
\end{aligned}$$

The two state variables a and b are obtained when the Moore-Greitzer partial differential equation for the stall dynamics is projected onto the first Fourier mode $a(t)\cos(\theta) + b(t)\sin(\theta)$. The axisymmetric compressor characteristic is $\psi_c(\Phi) = k_0 + k_1\Phi + k_2\Phi^2 + k_3\Phi^3$ and $\psi_c'(\Phi)$, $\psi_c''(\Phi)$, and ψ_c''' are its derivatives with respect to Φ. The model parameters l_c, B, μ, m, and λ are all positive constants. The mean value of the bleed flow is assigned by $\bar{\Phi}_b$ and the first discrete spatial Fourier mode of the bleed flow $C_a(t)\cos(\theta) + C_b(t)\sin(\theta)$ is assigned by C_a and C_b. The three variables $\bar{\Phi}_b$, C_a and C_b are independently set by the bleed valves, and in this control study we employ them as control variables $u = [\bar{\Phi}_b \; C_a \; C_b]^T$. When the bleed valves are closed, $\bar{\Phi}_b = C_a = C_b = 0$ and the model reduces to the original Moore-Greitzer model.

The linearization of the model (2.1)-(2.4) about any equilibrium on the characteristic $\psi_c(\Phi)$ appears as two decoupled subsystems:

$$A = \begin{bmatrix} A_1 & 0 \\ 0 & A_2 \end{bmatrix}, \quad B = \begin{bmatrix} B_1 & 0 \\ 0 & B_2 \end{bmatrix}$$

We refer to (2.1)-(2.2) as the surge subsystem and (2.3)-(2.4) as the stall subsystem. Both pairs (A_1, B_1) and (A_2, B_2) are controllable at all equilibria of interest. It follows that the full system (2.1)-(2.4) is locally controllable.

In the surge subsystem, the characteristic $\psi_c(\Phi)$ is the locus of equilibrium values for the mass flow Φ, and the pressure rise Ψ. A desired equilibrium is selected by adjusting the throttle coefficient K_T. Increasing the value of K_T corresponds to closing the throttle, which decreases the mass flow Φ and increases the pressure rise Ψ.

The cubic characteristic $\psi_c(\Phi)$ has one local maximum (peak). To the right of the peak, the equilibria are locally stable without feedback. To the left of the peak, the equilibria are unstable. The surge subsystem describes the fluid in the plenum as a nonlinear spring. Under certain conditions, the compressor enters a surge limit cycle and undergoes large oscillations in Φ and Ψ that often include negative values of Φ. When the flow reverses, engines typically "flame-out" and cease to function.

In the stall subsystem (2.3)-(2.4), the real part of the eigenvalues of A_2 is $\psi_c'(\Phi_e)/(\mu+m)$. To the left of the peak, these eigenvalues are unstable because the slope of the characteristic $\psi_c'(\Phi_e)$ is positive. The resulting instability known as "rotating stall" involves oscillations in a and b which are damaging to the engine and reduce the pressure rise across the compressor.

Whenever convenient, we denote the state vector by x, its equilibrium by x_e and $\tilde{x} = x - x_e$. We require the equilibrium value of the control u to be zero.

3 Control Design

The compressor's steady state performance is determined by the operating point on the characteristic $\psi_c(\Phi)$. The highest pressure rise Ψ, and hence, the best steady state performance is achieved at the peak of $\psi_c(\Phi)$. However, the peak is not a stable equilibrium of the uncontrolled system. Our design objective is to stabilize the peak and provide as large a region of attraction as possible. In addition to steady state performance, this objective aims to improve engine operability with respect to acceleration and inlet distortion.

In [13] we used the Linear Quadratic Regulator (LQR) and L_gV methodologies to design a control law for 2D bleed valves. The LQR control law $u = -R^{-1}B^TP\tilde{x}$ minimizes the cost functional $\int_0^\infty (x^TQx + u^TRu)dt$ for the linearization of (2.1)-(2.4). The matrix P is the positive definite solution of the Algebraic Ricatti Equation (ARE) $A^TP + PA - PBR^{-1}B^TP + Q = 0$. The solution P exists because the pair (A, B) is controllable. Eveker *et al* [8] and Krstic *et al* [17] have highlighted the importance of maintaining a tight control of the mass flow Φ. We achieve this by placing a high penalty on the mean flow error $\tilde{\Phi} = \Phi - \Phi_e$. The control cost R is also set relatively high because the bleed valves are capable of bleeding only 20% of the mass flow.

The L_gV framework extends the LQR design by including the nonlinearities of the control input matrix $g(x)$. For a control affine model of the form $\dot{x} = f(x) + g(x)u$, the L_gV controller employs a control Lyapunov function (CLF). Our candidate CLF is the optimal value function $V(\tilde{x}) = \tilde{x}^TP\tilde{x}$ from the LQR design, because it satisfies the CLF condition that

$$L_fV = \tilde{x}^T(A^TP + PA)\tilde{x} = -\tilde{x}^TQ\tilde{x} \leq 0$$

$$\text{whenever } L_gV = 2\tilde{x}^TPB = 0.$$

Thus, $V(\tilde{x})$ is guaranteed to be a CLF at least where the linearization is a valid approximation of the system. The corresponding L_gV control is $u = -2k_n(P\tilde{x})^Tg(x)$. Our choice for k_n is to match the linearization to the LQR controller by assigning $k_n = \frac{1}{2}R^{-1}$. The resulting nonlinear control is

$$u = -R^{-1}g^T(x)(P\tilde{x}) \tag{3.5}$$

The linearization of this control law is identical to the LQR design and is *locally* optimal.

We now analyze stability properties of the closed loop system (2.1)-(2.4) with the L_gV controller. In the experiments described in Section 6, there is little variation in the pressure Ψ. For this reason, we focus on the $(\tilde{\Phi}, J)$ plane of the state space at the peak pressure Ψ_e, where $J = \sqrt{a^2 + b^2}$ is the amplitude of the first mode of rotating stall and $\tilde{\Phi}$ is mean flow error $\Phi - \Phi_e$ so that the bottom right corner of the plane corresponds to the peak of the compressor characteristic. In this plane, we examine the compressor's stability with respect to mean and first mode flow disturbances that are captured by different initial values of these variables.

As mentioned above, Φ is the most critical state variable to control. When a trajectory passes to the left of the peak, $\dot{\Phi} < 0$. In order for this trajectory to return to the peak, $\dot{\Phi}$ must first be made zero, and then positive by the control law. Because of control saturation, there is a boundary beyond which $\dot{\Phi}$ can not be made positive and the system enters surge or rotating stall. To estimate this boundary, we saturate the controls at $C_a = C_b = \max(C_a)$ which implies $\bar{\Phi}_b = \frac{1}{2}\max(\bar{\Phi}_b)$. With this maximum control effort we plot in Figure 1 the manifold $\dot{\Phi} = 0$ which indicates the boundary beyond which the destabilizing dynamics are more powerful than the saturated controls. This boundary is independent of a Lyapunov function or control law, and serves as a rough estimate for the region attraction possible with feedback control.

4 Experimental Facility

The LS3 experimental compressor was designed at United Technologies Research Center. A drive motor spins the rotor 2400 rpm. To better approximate the surge and stall dynamics of industrially relevant compressors, Protz [5] increased the B parameter by increasing the volume of the plenum. A ring of butterfly-type valves is located downstream of the last compressor stage at a distance equal to half a compressor radius. The actuation ring has only four valves to represent the bleed ports that already exist in industrial engines. These bleed valves are able to bleed approximately 20% of the mass flow. Each valve is driven by an independent motor with a bandwidth of 60 Hz.

An array of eight hotwires is equally distributed

around annulus to measure the unsteady mass flow. The array is located in the first stage rotor-stator interstage gap at the mid-span of the annulus. The hotwires have a bandwidth of 50 kHz. The signals generated by these sensors are averaged to produce the mean flow Φ and the discrete Fourier transform (DFT) is used to generate the real and imaginary components of the first mode stall cell, a and b. The unsteady plenum pressure is measured with a strain-gauge pressure sensor located at the center of a plenum side wall. Its natural frequency is 28 kHz.

5 Implementation Constraints

The physical limitations of bleed valves play a significant role in compressor stabilization. Bleed valve area is nonnegative and finite. The bleed valve motor time lag and rate constraint dictate how quickly a valve can be opened. Because the control variables compete for the available bleed flow of the individual valves, a strategy is needed to allocate individual valve openings to the controls $\bar{\Phi}_b$, C_a and C_b.

To analyze the actuator constraints, the control variables C_a, C_b, and $\bar{\Phi}_b$ must first be related to the bleed flow $\phi_b(\theta)$ exiting the valves. Experimental measurements of the compressor mass flow under the influence of the valves indicate that a square pulse with an amplitude of v_i (where i designates the valves 1 through 4) and a width of $\Delta\theta$ is a reasonable approximation for the spatial shape of the mass flow bled by a valve. The relationship between the physical valve area v_a and the valve mass flow v_i can not be measured directly. Instead it is estimated from the equation $v_i = \sqrt{\frac{\psi_b}{v_a}}$ where ψ_b is the difference between the compressor and ambient pressures. The square pulse decays slightly due to the gap between the valves and the last stage of the compressor. For this reason, a delay is included in the Fourier approximation for the bleed flow due to *one* valve, $\phi_b(\theta) \approx v_0 + e^{-1}(a_v \cos(\theta) + b_v \sin(\theta))$. The coefficients are

$$v_0 = \frac{\Delta\theta}{2\pi} v_i \tag{5.6}$$

$$a_v = \frac{2v_i}{\pi} \sin(\frac{\Delta\theta}{2}) \cos(\bar{\theta}) \tag{5.7}$$

$$b_v = \frac{2v_i}{\pi} \sin(\frac{\Delta\theta}{2}) \sin(\bar{\theta}) \tag{5.8}$$

and $\bar{\theta}$ is the location of the valve in the annulus of the compressor. The value of $\Delta\theta$ was measured as 26^o. Thus the bleed flows of adjacent valves do not overlap and we assume that their influence is independent of each other. We add their individual effects and substitute the corresponding valve locations $\bar{\theta} = 0,\ \frac{\pi}{2},\ \pi,\ \frac{3\pi}{2}$ to obtain the Fourier approximation

$$\phi_b(\theta) \approx \frac{\Delta\theta}{2\pi}\Sigma v_i + e^{-1}\left(\frac{2}{\pi}\sin(\frac{\Delta\theta}{2})\right) \times \left[(v_1 - v_3)\cos\theta + (v_2 - v_4)\sin\theta\right]$$

Matching the above expression to the bleed flow assumed by the model $\phi_b = \bar{\Phi}_b + C_a(t)\cos(\theta) + C_b(t)\sin(\theta)$, we see that

$$\bar{\Phi}_b = \frac{\Delta\theta}{2\pi}\Sigma v_i \tag{5.9}$$

$$C_a = e^{-1}\left(\frac{2}{\pi}\sin(\frac{\Delta\theta}{2})\right)(v_1 - v_3) \tag{5.10}$$

$$C_b = e^{-1}\left(\frac{2}{\pi}\sin(\frac{\Delta\theta}{2})\right)(v_2 - v_4) \tag{5.11}$$

Equations (5.9) and (5.10) reveal that the surge control variable $\bar{\Phi}_b$ is proportional to the sum of the valve openings, while the stall control variables C_a and C_b are proportional to the difference of opposing valve openings. Thus, the constraint $0 \le v_i \le \bar{v}$ results in constraints on the relationship between the mean bleed $\bar{\Phi}_b$ and the first mode bleeds C_a and C_b. While C_a assumes positive and negative values, $\bar{\Phi}_b$ must always be positive. We also note that the maximum values of $\bar{\Phi}_b$ and C_a do not coincide. In fact, the the maximum of $\bar{\Phi}_b$ requires C_a to be zero. Thus, to reach their maximum levels, $\bar{\Phi}_b$ and C_a compete for different values of the individual bleed valve flows v_i.

It is known that at 2400 RPM, the LS3 is more likely to stall than surge. This suggests that in the above competition for the available bleed, priority should be given to the stall controls C_a and C_b. It is of interest to examine if this intuition can be confirmed with our control Lyapunov function V. A quadratic program was used to determine which values of $\bar{\Phi}_b$, C_a and C_b minimize the derivative $\dot{V}$ of the Lyapunov function. Indeed, the optimal solution saturates the stall controls very near the operating point and subordinates $\bar{\Phi}_b$ to make this saturation possible. Thus, priority is given to the stall controls C_a and C_b irrespective of the mean

bleed command $\bar{\Phi}_b$. Then, if there is freedom to adjust $\bar{\Phi}_b$, it is set as close to the command as possible.

The bandwidth of the valves was measured to be 60 Hz and the rate limit was measured at $450^o/\text{s}$. The surge instability of the LS3 is about 2 Hz and the valves are fast enough for stabilization. The first mode of rotating stall, on the other hand, has a frequency of 20 Hz and is dangerously close to the bandwidth of the valves.

Control of rotating stall offers a unique opportunity to take into account and overcome the dynamic limitations of the bleed valves. If both the time lag of the valves and the velocity of the stall cell are known, then the circumferential distance that the stall cell travels in that time is also known. In this way a *lag in the time domain* can be compensated by a *lead in the spatial domain* with the following equation

$$\text{(stall cell speed)} \times \text{(valve time lag)} = \text{spatial phase lead}$$

Thus, it is possible to calculate the necessary spatial phase lead to add to the valve commands so that the stall actuation is in phase with the stall cell itself.

6 Experimental Evaluation

The LS3 can not be accelerated because it does not have a combustor or a turbine. However, a back pressure similar to accelerating the compressor is achieved with a disturbance valve in the plenum. When the compressor is run with the valve open, closing it quickly drives the compressor to a lower mass flow near the peak of the compressor characteristic. The resulting transient overshoots the peak and then, if stable, returns to the peak. Varying overshoot magnitudes are generated by different levels of the disturbance valve command. In this way, the region of attraction of the peak is measured with respect to the mean flow coordinate.

Measuring the region of attraction with respect to the amplitude of the first mode of rotating stall is not as straightforward because the disturbance valve can not induce stall directly. When the compressor is operating to the left of the peak, stall

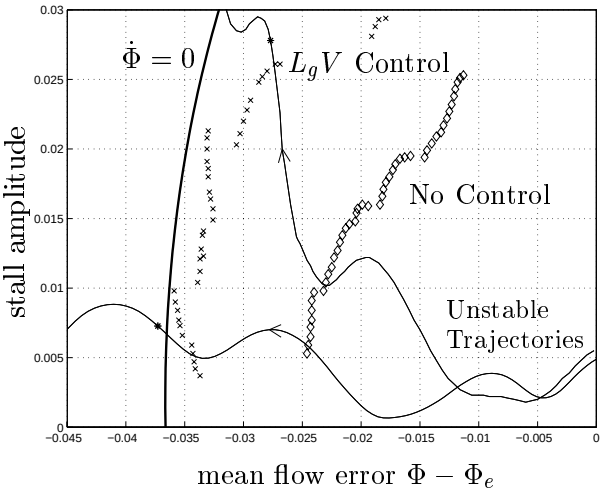

Figure 1: Experimental data indicating the region of attraction for the LS3

is spontaneously induced. By introducing a delay between the time that the disturbance is commanded and the time that the control is turned on, it is possible to test if the compressor recovers from various amplitudes of rotating stall. In this way it is possible to indirectly generate several initial conditions to the left of the peak and measure a portion of the compressor's region of attraction. The above experimental procedure was carried out on the LS3 compressor. The results of the experiments are displayed in the $(\tilde{\Phi}, J)$ plane where $\tilde{\Phi} = \Phi - \Phi_e$ and $J = \sqrt{a^2 + b^2}$.

Points on stable trajectories that converged to the peak define the region of attraction. The experimentally obtained data points on the boundary of this region are plotted in Figure 1. Open loop experimental data are indicated with a $\diamond$ and an "x" is used for experiments with the L_gV controller. The data show that the L_gV controller extends the region of attraction almost 50% beyond the open loop data.

To confirm the stability boundary, two unstable trajectories are also plotted in Figure 1. The points where the control is turned on are marked with an "*". The actual stability boundary must lie between the stable and unstable points. The proximity of these points indicates that the stability boundary is close to the stable L_gV data.

In Section 2 the manifold $\dot{\Phi} = 0$ was used to estimate the largest region of attraction achievable with any controller. In Figure 1, the proximity of this manifold to the data indicates that the L_gV

controller is a good representative of the increased stability that can be achieved with feedback control.

7 Conclusions

We have implemented a nonlinear L_gV control law for 2D bleed actuation on a low speed three stage compressor. The region of attraction guaranteed by this controller is significantly larger than that of the open loop system. In fact, the nonlinear controller nearly matches an estimate of the largest region of attraction achievable with any controller.

References

[1] J. Paduano, L. Valvani, A. Epstein, E. Greitzer, and G. Guenette, "Modeling for control of rotating stall", *Automatica*, vol. 30, no. 9, pp. 1357–1373, 1994.

[2] J. Paduano, A. Epstein, L. Valvani, J. Longley, E. Greitzer, and G. Guenette, "Active control of rotating stall in a low speed axial compressor", *J. of Turbomachinery*, vol. 115, pp. 48–56, January 1993.

[3] C. Freeman, A. Wilson, I. J. Day, and M. Swinbanks, "Experiments in active control of stall on an aeroengine gas turbine", Orlando, June 1997, ASME Turbo Expo.

[4] H. Weigl, J. Paduano, L. Frechette, E. Greitzer, M. Bright, and A. Strazisar, "Active stabilization of rotating stall in a transonic single stage axial compressor", Orlando, June 1997, ASME Turbo Expo, number 97-GT-411.

[5] J. Protz, "Nonlinear active control of rotating stall and surge", Master's thesis, MIT, 1995.

[6] B. Behnken and R. Murray, "Active control of an axial flow compressor via pulsed air injection", *J. of Turbomachinery*, to appear.

[7] H.-H. Wang, S. Yeung, and M. Krstic, "Experimental application of extremum seeking on an axial-flow compressor", in *American Control Conference*. IEEE, 1998, pp. 1989–93.

[8] K. M. Eveker, D. L. Gysling, C. N. Nett, and O. P. Sharma, "Integrated control of rotating stall and surge in aeroengines", Orlando, April 1995, SPIE Conference on Sensing, Actuation, and Control in Aeropropulsion.

[9] O. Badmus, S. Chowdhury, K. Eveker, C. Nett, and C. Rivera, "A simplified approach for control of rotating stall. part 2: Experimental results", in *Joint Propulsion Conference*. AIAA, 1993, Paper No. 93-2234.

[10] B. Behnken and R. Murray, "Combined air injection control of rotating stall and bleed valve control of surge", Albuquerque, June 1997, American Control Conference, pp. 987–992.

[11] S. Yeung and R. Murray, "Nonlinear control of rotating stall using axisymmetric bleed with continuous air injection on a low-speed, single stage, axial compressor", in *Joint Propulsion Conference*. AIAA, 1997.

[12] F. Willems and B. Jager, "Modeling and control of compressor flow instabilities", *IEEE Control Systems*, vol. 19, no. 5, pp. 8–18, December 1999.

[13] D. Fontaine, S. Liao, P. Kokotovic, and J. Paduano, "Two dimensional, nonlinear control of an axial flow compressor", IEEE Conference on Control Applications, 1999.

[14] J. Kerrebrock, *Aircraft Engines and Gas Turbines*, The MIT Press, 1992.

[15] T. Hynes and E. Greitzer, "A method for assesing the effects fo circumferential distortion on compressor stability", *J. of Turbomachinery*, vol. 109, pp. 371, 1987.

[16] F. K. Moore and E. M. Greitzer, "A theory of post-stall transients in axial compression systems: Part I - development of equations", *Journal of Engineering for Gas Turbines and Power*, vol. 108, pp. 68–76, January 1986.

[17] M. Krstić, D. Fontaine, P. Kokotovic, and James Paduano, "Useful nonlinearities and global bifurcation control of jet engine stall and surge", *IEEE Trans. Auto. Contr.*, vol. 43, no. 12, December 1998.